INTERFACE

rsif.royalsocietypublishing.org

Research

Cite this article: Fitzer SC, Zhu W, Tanner KE, Phoenix VR, Kamenos NA, Cusack M. 2015 Ocean acidification alters the material properties of *Mytilus edulis* shells. *J. R. Soc. Interface* **12**: 20141227.
http://dx.doi.org/10.1098/rsif.2014.1227

Received: 5 November 2014
Accepted: 5 December 2014

Subject Areas:
environmental science, biogeochemistry, biomaterials

Keywords:
biomineralization, ocean acidification, temperature, mussels, CO_2, multiple stressors

Author for correspondence:
Susan C. Fitzer
e-mail: susan.fitzer@glasgow.ac.uk

Electronic supplementary material is available at http://dx.doi.org/10.1098/rsif.2014.1227 or via http://rsif.royalsocietypublishing.org.

THE ROYAL SOCIETY PUBLISHING

Ocean acidification alters the material properties of *Mytilus edulis* shells

Susan C. Fitzer[1], Wenzhong Zhu[3], K. Elizabeth Tanner[2], Vernon R. Phoenix[1], Nicholas A. Kamenos[1] and Maggie Cusack[1]

[1]School of Geographical and Earth Sciences, and [2]School of Engineering, University of Glasgow, Glasgow G12 8QQ, UK
[3]School of Engineering, University of the West of Scotland, Paisley PA1 2BE, UK

SCF, 0000-0003-3556-7624; WZ, 0000-0002-2669-9177; KET, 0000-0003-2257-0218; VRP, 0000-0002-8682-5200; NAK, 0000-0003-3434-0807; MC, 0000-0003-0145-1180

Ocean acidification (OA) and the resultant changing carbonate saturation states is threatening the formation of calcium carbonate shells and exoskeletons of marine organisms. The production of biominerals in such organisms relies on the availability of carbonate and the ability of the organism to biomineralize in changing environments. To understand how biomineralizers will respond to OA the common blue mussel, *Mytilus edulis*, was cultured at projected levels of pCO_2 (380, 550, 750, 1000 µatm) and increased temperatures (ambient, ambient plus 2°C). Nanoindentation (a single mussel shell) and microhardness testing were used to assess the material properties of the shells. Young's modulus (E), hardness (H) and toughness (K_{IC}) were measured in mussel shells grown in multiple stressor conditions. OA caused mussels to produce shell calcite that is stiffer (higher modulus of elasticity) and harder than shells grown in control conditions. The outer shell (calcite) is more brittle in OA conditions while the inner shell (aragonite) is softer and less stiff in shells grown under OA conditions. Combining increasing ocean pCO_2 and temperatures as projected for future global ocean appears to reduce the impact of increasing pCO_2 on the material properties of the mussel shell. OA may cause changes in shell material properties that could prove problematic under predation scenarios for the mussels; however, this may be partially mitigated by increasing temperature.

1. Introduction

Ocean acidification (OA) poses a threat to those marine organisms that produce calcium carbonate shells and exoskeletons. As anthropogenic carbon dioxide enters the oceans, the increasing pCO_2 reduces the carbonate available to marine organisms [1]. Projections of increases in future pCO_2 have stimulated investigations to understand the impact on calcifying marine organisms. Reductions in growth and calcification rates are just a few of the physiological impacts of OA [2–5]. While experimental impacts of OA on marine organisms tend to focus on the physiological responses, two studies [6,7] examine the impact on the ultrastructure of these protective exoskeletons of the oyster *Crassostrea virginica* and the clam *Mercenaria mercenaria*. These studies report reduced microhardness after 15 weeks in OA conditions [6] and reduced fracture resistance in the juvenile eastern oyster *C. virginica* after 11 weeks under OA conditions [7]. Shell strength [8] and byssal thread strength have also been examined as a means to address the mechanical integrity of mussel shells and byssal threads [9]. Long-term and, if possible, multi-generational studies are vital to understand the possibility of acclimation or even adaptation of marine organisms to OA. Owing to difficulties in laboratory cultures, only a few such studies exist [10,11].

The common blue edible mussel, *Mytilus edulis*, is an economically important mollusc with a shell comprising two calcium carbonate polymorphs: calcite (prismatic layer) and aragonite (nacreous layer or mother of pearl). The inner aragonite is potentially more vulnerable to reduced carbonate

saturation states projected with increasing OA [1] than the outermost calcite, which is the more stable of the calcium carbonate polymorphs.

This study examines the impact of OA on the material properties of the common blue mussel (*M. edulis*) shell using nanoindentation and fracture toughness measurements.

2. Material and methods

2.1. Mussel collection and culture

Mussels (*M. edulis*) were obtained from Loch Fyne, Argyll, UK (Loch Fyne Oysters Ltd) during October 2012. Mussels (1 year old) were placed into experimental tanks (6 l) supplied with natural filtered (1 µm and UV) seawater at Loch Fyne temperatures (7°C) and ambient pCO_2 (approx. 380 µatm). Mussel shells were stained prior to experimental culture using seawater containing the fluorescent dye calcein (150 mg l^{-1} calcein C0875-25g; Sigma–Aldrich) for 6 h [12]. Mussels were rinsed thoroughly in seawater and placed back in experimental tanks. Mussels were fed 10 ml of cultured microalgae (five species of algae, *Nannochloropsis* sp., *Tetraselmis* sp., *Isochrysis* sp., *Pavlova* sp., *Thalassiosira weissflogii* (stock from Reefphtyo, UK)) per tank every other day [12]. Feeding was conducted during a two-week acclimation and throughout the experimental period. The feeding regime (10 ml of approx. 2.8 million cells ml^{-1} algae culture) was equivalent to approximately 4666 cells ml^{-1} during experimental culture; this is sufficient to allow for growth under OA [5,13]. Each experimental tank contained 30 mussels; this was the appropriate number of mussels per 6 l experimental tank to maintain sufficient dissolved oxygen (DO) levels (tested prior to experiment).

2.2. Environmental conditions

Seasonal experimental temperatures and day length (light) mirrored those at the collection site. Experiments were conducted at 380, 550, 750 and 1000 µatm pCO_2 at ambient temperature and ambient plus 2°C, reflecting the seasonal changes under global warming conditions (380, 750 and 1000 µatm at ambient plus 2°C). Seawater pCO_2 concentrations were brought to experimental levels (380, 550, 750 and 1000 µatm pCO_2) over a one-month period. CO_2 was mixed into air lines supplying all experimental tanks [12,14]. Gas concentrations were logged continuously using LI-COR Li-820 CO_2 gas analysers (table 1) [12]. Seawater was topped up with a mixture of seawater and freshwater once a week to simulate fresh water pulses experienced by mussels in their natural environment. This is reflected in calcite (Ω Ca) and aragonite (Ω Ar) saturation states, which are similar to other OA studies examining brackish water environments [15] and the natural variability present at the collection site (table 1). Seawater was sampled in replicate for three sites around the mussel farming site of Loch Fyne for analysis of carbonate chemistry during one day in August compared with the experimental period of November to June [12]; the averages and lowest alkalinity values are presented in table 1. Seawater salinity, temperature and DO were checked daily and recorded once a week (YSI Pro2030). Seawater samples were collected (once per month) and spiked with 50 µl of mercuric chloride for subsequent total alkalinity (A_T) analysis via semi-automated titration (Metrohm 848 Titrino Plus) [16] combined with spectrometric analysis using bromocresol indicator [17] (smart pH cuvettes, Ocean Optic Ltd; Hach DR 5000 UV–vis). Certified seawater reference materials for oceanic CO_2 (batch 123; Scripps Institution of Oceanography, University of California, San Diego, CA, USA) were used as standards to quantify the error of analysis (measured 2141 ± 54 µmol kg^{-1}, certified reference material (CRM) value 2225.21 ± 0.14 µmol kg^{-1}) [16]. Seawater

Table 1. Experimental seawater chemistry parameters: salinity, dissolved oxygen (DO), pCO_2, total alkalinity (A_T ± standard deviation from the mean). Loch Fyne natural seawater chemistry parameters. Salinity, DO and temperature are averages collected manually throughout experiments, and pCO_2 given is the averaged values logged throughout the six months of experiments (logging every 5 min) using LI-COR software. Bicarbonate (HCO_3^-) and carbonate (CO_3^{2-}), calcite saturation state (Ω Ca) and aragonite saturation state (Ω Ar) were calculated from measured parameters using CO_2Sys.

experimental condition	salinity (ppt)	DO (%)	temperature (°C)	pCO_2 (µatm)	A_T (µmol kg^{-1})	HCO_3^- (µmol kg^{-1})	CO_3^{2-} (µmol kg^{-1})	Ω Ca	Ω Ar
380 µatm ambient	32.78 ± 1.42	95.58 ± 1.84	9.40 ± 0.36	375.62 ± 9.69	635.24 ± 28.93	590.3	11.9	0.29	0.18
380 µatm ambient plus 2°C	36.10 ± 1.45	97.54 ± 2.40	11.58 ± 0.69	375.62 ± 9.69	703.05 ± 78.66	641.6	16.7	0.39	0.25
550 µatm ambient	32.74 ± 1.56	99.04 ± 2.19	10.01 ± 0.56	553.59 ± 62.65	970.76 ± 186.48	908.9	19.7	0.47	0.30
750 µatm ambient	28.42 ± 4.07	98.64 ± 4.78	10.28 ± 0.34	768.74 ± 41.63	753.64 ± 55.16	725.7	8.4	0.21	0.13
750 µatm ambient plus 2°C	36.58 ± 3.84	97.76 ± 2.55	12.34 ± 0.43	768.74 ± 41.63	681.39 ± 41.61	649.0	8.7	0.21	0.13
1000 µatm ambient	34.18 ± 4.58	98.66 ± 1.97	10.23 ± 0.40	1132.53 ± 31.74	698.32 ± 5.77	678.2	5.6	0.13	0.08
1000 µatm ambient plus 2°C	37.26 ± 2.14	97.55 ± 1.98	12.04 ± 0.35	1132.53 ± 31.74	642.06 ± 27.60	621.3	5.4	0.13	0.08
Loch Fyne variability	19.33 ± 7.46	99.36 ± 12.99	15.70 ± 4.15	341.17 ± 102.57	1261.95 ± 416.39	1170.56 ± 430.42	34.37 ± 18.99	0.88 ± 0.47	0.52 ± 0.29
Loch Fyne (lowest total alkalinity values)	17.80	116	12.80	250.8 ± 3.7	876.10 ± 12.62	798.39 ± 11.75	29.19 ± 0.44	0.68 ± 0.01	0.39 ± 0.01

Table 2. Young's modulus (E) and hardness (H) average values for each pCO_2 condition presented for calcite new growth (NG) samples and newest aragonite samples containing calcite older growth (OG). Standard deviation (s.d.) and % coefficient of variation (%COV) are reported for the 24–45 indents per mussel shell calcite NG, 9–14 indents per mussel shell aragonite and 25–40 indents per mussel shell calcite OG.

pCO_2 condition	mineral	E (GPa)	s.d.	%COV	H (GPa)	s.d.	%COV
380	calcite NG	69.60	1.65	2.37	2.76	0.11	4.06
550	calcite NG	70.39	1.62	2.30	2.97	0.13	4.32
750	calcite NG	80.52	1.66	2.07	2.88	0.17	5.87
1000	calcite NG	73.03	3.65	5.00	2.84	0.09	3.30
380 + 2°C	calcite NG	68.10	2.40	3.52	2.83	0.18	6.52
750 + 2°C	calcite NG	72.15	2.78	3.85	2.77	0.14	5.00
1000 + 2°C	calcite NG	70.35	1.28	1.82	2.74	0.08	2.94
380	aragonite	91.92	3.89	4.23	4.06	0.26	6.31
550	aragonite	84.04	2.47	2.94	4.04	0.26	6.31
750	aragonite	81.34	5.69	7.00	3.78	0.32	8.57
1000	aragonite	87.67	3.88	4.43	3.98	0.32	7.93
380 + 2°C	aragonite	81.69	2.83	3.46	4.39	0.20	4.52
750 + 2°C	aragonite	82.72	4.87	5.89	3.94	0.24	6.07
1000 + 2°C	aragonite	82.26	3.62	4.40	3.95	0.41	10.27
380	calcite OG	72.30	2.01	2.78	2.83	0.13	4.76
550	calcite OG	71.94	2.21	3.07	2.93	0.11	3.90
750	calcite OG	74.90	1.63	2.17	3.17	0.13	4.15
1000	calcite OG	76.81	1.90	2.47	3.12	0.13	4.19
380 + 2°C	calcite OG	71.18	2.25	3.16	3.11	0.13	4.07
750 + 2°C	calcite OG	75.77	2.61	3.44	3.20	0.13	4.03
1000 + 2°C	calcite OG	70.97	2.22	3.13	3.05	0.16	5.14

A_T, salinity, temperature and pCO_2 were used to calculate other seawater parameters using CO_2SYS [18] (table 1).

2.3. Shell preparation

Mussels sampled after six months of experimental culture were dissected, cleaned, oven dried by incubation at 60°C for 48 h and then embedded in epoxy resin (EpoxyCure, Buehler) blocks. Embedded shells were sliced transversely using a diamond trim saw blade to section the whole length of the shell. New growth was determined through calcein staining of growth bands at the start of experimental culture as detailed in [12]; any growth prior to this stained growth band was named old growth, which occurred prior to experimental culture. The new growth at the outer edge of the shell (containing newest calcite) and towards the newest aragonite formation (containing both newest aragonite and older calcite) was sectioned and mounted in a resin block before polishing the cut edge of the shell. Resin blocks were ultra-polished using aluminium oxide (0.3 and 1 µm) and colloidal silica (0.6 µm).

2.4. Nanoindentation

Materials properties were assessed by establishing hardness (H) and Young's modulus (E) using a nanoindenter G200 system (Agilent Technologies) fitted with a diamond Berkovich tip. The average values for E and H over the indentation depth range of 150–350 nm are given for a single mussel shell. Parameters and images of nanoindentation are provided for each analysed sample (electronic supplementary material, figures and tables),

$$E = \frac{\text{stress}}{\text{strain}} = \frac{\sigma}{\varepsilon},$$

where E is Young's modulus, σ is stress exerted on an object and ε is the strain. When E is higher the sample is stiffer; the values obtained for the mussel shell are similar to those expected for a highly mineralized tissue such as enamel [19].

2.5. Microindentation measurement of fracture toughness

Fracture toughness of the mussel shells was assessed on two separate individual mussels per group using Vickers Hardness microindentation (Micro Vickers 401 MVA, Wilson Wolpert Co., Ltd) testing. Three indents were made per region (calcite/aragonite) for each mussel shell and averages reported ± the standard deviation from the mean. A load of 0.5 kg was applied for 10 s, the lengths of the diagonals of the indent were measured to calculate the Vicker's hardness (H) and the length of the cracks developed from the corners of the indent measured to determine fracture toughness (K_{IC}) using the equation from [20–22]

$$K_{IC} = 0.16\left(\frac{c}{a}\right)^{-1.5} H(a)^{0.5},$$

where c is the average length of the cracks obtained from the tips of the Vickers indent (micrometres), a is half the average length of the diagonal of the Vickers indent and H is the Vickers hardness (MPa).

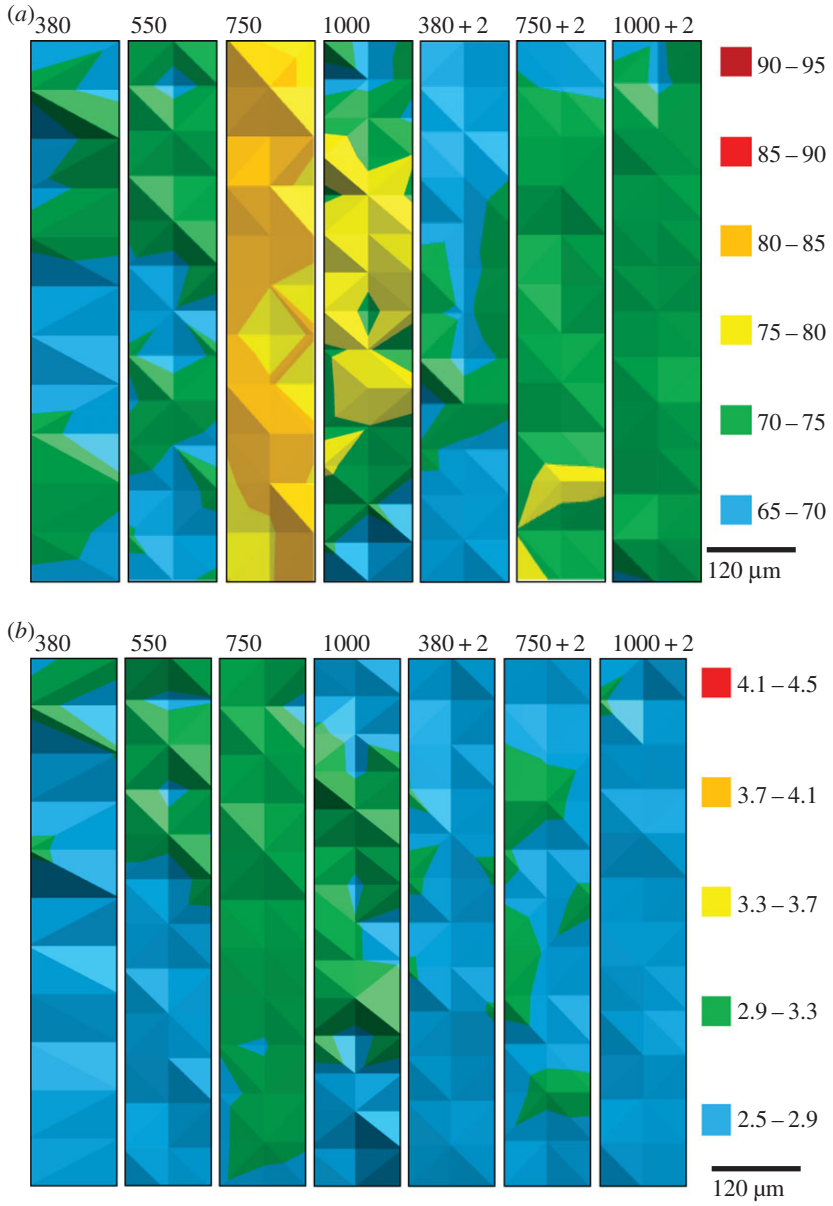

Figure 1. Maps of elasticity and hardness of new calcite growth as determined by nanoindentation on a single mussel shell; (*a*) Young's modulus, *E* (GPa), and (*b*) hardness, *H* (GPa). Shell interior to the top of each map. Colour legends are given in units of GPa for each figure where red is stiffer and harder. 380, 550, 750 and 1000 indicate µatm pCO_2 in which the shell grew; 380 + 2, 750 + 2, and 1000 + 2 indicate that experimental temperature was 2°C above ambient.

2.6. Statistical testing

Hardness and elastic modulus were measured for each indent mapped across each mussel shell (one shell per treatment); this was automatically calculated using the TestWorks nanoindentation software. For statistical analysis, the calculated values for each indent (9–45 indents per region per shell) were averaged across the individual shell for each treatment. Standard deviation and percentage coefficient of variation were reported for the mean values (table 2). Microhardness testing for fracture toughness was performed on two separate individual mussels (electronic supplementary material, table S15). These data indicated that hardness does not significantly differ between individual mussels (one-way ANOVA, hardness versus mussel individual, $p = 0.713$, $F = 0.14$, d.f. = 1), allowing for the presentation of the higher resolution nanoindentation data provided for only one mussel at much higher spatial resolution. Fracture toughness was measured for each indent and averaged across the indents for each part of the mussel shell. General linear model ANOVA analyses were used to assess the significance of the effect of pCO_2 and increased temperature on shell fracture toughness with assumptions of normality and homogeneity of variance being met.

3. Results

3.1. Newest calcite growth

Mussel shells with the newest calcite growth within the six months of experimental culture had harder and stiffer (i.e. having higher *H*- and *E*-values) calcite when grown under increased pCO_2. The growth of the mussels from 1 year old during the course of the six-month experimental culture was determined in a previous publication [12], ranging from over 1 to 3 mm, and dependent on the experimental pCO_2 [12]. There are dramatic increases in *E* and *H* at 750 µatm pCO_2 compared with mussel shells grown at ambient 380 µatm pCO_2 (figure 1 and table 2). Increasing the temperature to ambient plus 2°C seems to reduce the

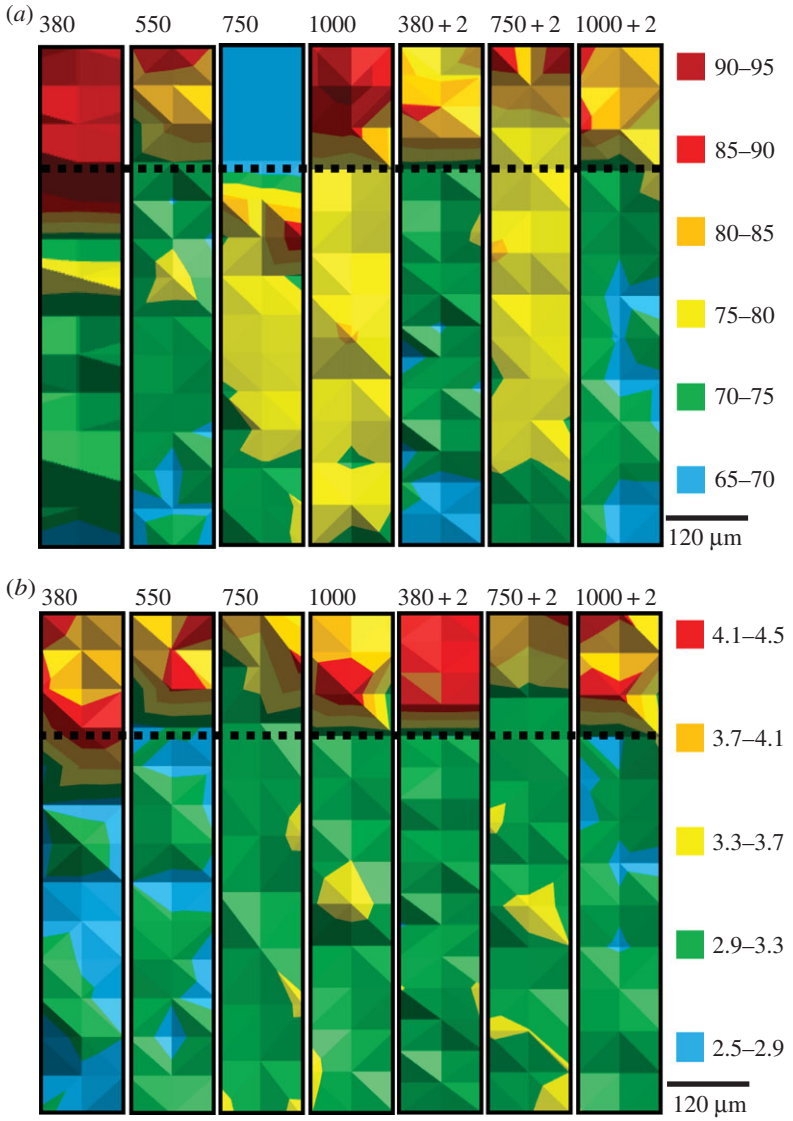

Figure 2. Maps of elasticity and hardness of calcite and aragonite as determined by nanoindentation on a single mussel shell; (*a*) Young's modulus, *E* (GPa), and (*b*) hardness, *H* (GPa). Aragonite at the top of the map, calcite at the bottom, the interface represented by the dotted line, i.e. shell interior at the top of each map as for figure 1. Colour legends are given in units of GPa for each figure where red is less elastic and harder. 380, 550, 750 and 1000 indicate µatm pCO_2 in which the shell grew; 380 + 2, 750 + 2, and 1000 + 2 indicate that experimental temperature was 2°C above ambient.

impact of the higher pCO_2 on *E* and *H*. This results from increased temperature alone (380 µatm pCO_2 + 2°C) generating less stiff calcite than ambient (380 µatm pCO_2), yet at higher pCO_2 values (750 and 1000 µatm pCO_2) increased temperature results in calcite that is stiffer than the 380 µatm pCO_2 + 2°C (figure 1 and table 2).

3.2. Newest aragonite growth

Nacre was harder and stiffer than calcite in mussel shells cultured under increased pCO_2 (figure 2). Increased pCO_2 up to 750 µatm resulted in less stiff, softer nacre (figure 2 and table 2). Mussel shells cultured under increasing temperature to ambient plus 2°C alone (380 µatm pCO_2 + 2°C) results in harder nacre, whereas this effect was diminished at higher pCO_2 values with elevated temperatures (750 and 1000 µatm pCO_2 + 2°C; figure 2 and table 2).

3.3. Older calcite growth

Older calcite growth was analysed using nanoindentation for comparison of the newest shell growth maintained during the six months of experimental culture. The older calcite was similarly harder and stiffer than the old calcite formed in the ambient pCO_2 value (380 µatm pCO_2; figure 2 and table 2). The exception to this is significantly less stiff old calcite in those mussel shells cultured under 550 µatm pCO_2 (figure 2).

3.4. Shell fracture toughness

Mussel shells were examined for shell fracture toughness using microindentation in two individual mussel shells for both older calcite and aragonite and newest calcite. The determined hardness confirmed trends seen by nanoindentation in the newest shell growth. Fracture toughness significantly decreased in those mussel shells cultured under 550 and 750 µatm pCO_2 ($p = 0.075$, $t = -1.83$, d.f. = 6 and $p = 0.005$, $t = -3.01$, d.f. = 6, respectively; figure 3). Combined temperature and pCO_2 reduced the impact on the fracture toughness on shells, with a significant increase in fracture toughness at each pCO_2 and increasing temperature to ambient plus 2°C ($p = 0.001$, $t = -3.70$, d.f. = 2; figure 3).

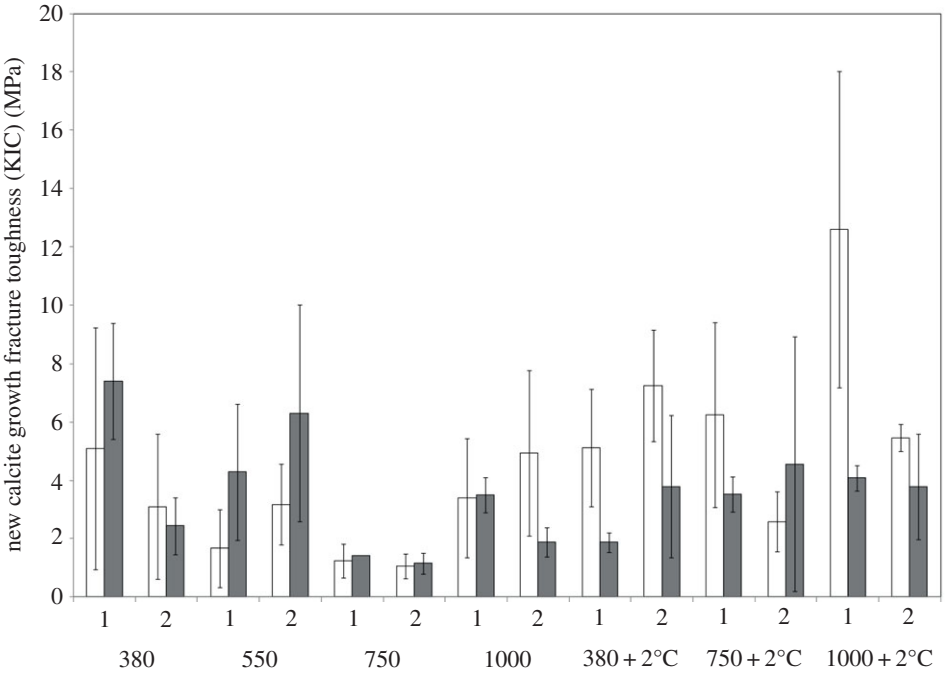

Figure 3. Fracture toughness for two individual mussels in newest calcite growth (white bars) and aragonite growth (grey bars). Fracture toughness is reported as the mean of three indents, error bars representing the standard deviation from the mean. 380, 550, 750 and 1000 indicate µatm pCO_2 in which the shell grew; 380 + 2, 750 + 2 and 1000 + 2 indicate that experimental temperature was 2°C above ambient.

4. Discussion

Mussel shells grown under increasing pCO_2 produce stiffer, harder calcite in the newest and older calcite growth. This suggests that the calcite is less elastic, or stiffer and harder, in elevated pCO_2 conditions, leading to an outer shell that is more brittle.

The mussel shell's reduced resistance to brittle fracture was confirmed by the quantification of the fracture toughness [20], with significant reductions in fracture toughness at 550 and 750 µatm (figure 3). Mussel shells grown under increasing pCO_2 would thus become more fragile, which may result in shells more likely to shatter under impact (similar *E* approx. 70–80 GPa) and thus being more vulnerable to breakage through predation. In the case of aragonite, the polymorph most vulnerable to reduced carbonate saturation under OA, fracture toughness is also reduced (figure 3) with increasing pCO_2, even though its hardness and *E* modulus are reduced. The aragonite polymorph was, however, prior to acidification much harder and stiffer than the calcite polymorph. Moderate pCO_2 (approx. 800 µatm) did not impact shell fracture toughness or microhardness of the clam, *M. mercenaria*, and oyster, *C. virginica*, shells [6], which differs from the findings presented here. However, in Ivanina *et al.* [6], shell growth under experimental culture could not be separated from growth present at the start of their experiments [6]. Limiting food supply combined with increasing pCO_2 has been shown to amplify resulting corrosion of the aragonite layer in *M. edulis* [13], and associated changes in microstructure could result in changes to material properties [13]. During this study, *M. edulis* were fed a sufficient food supply of approximately 5000 cell ml^{-1} of algae compared with the 1600–2000 cell ml^{-1} of Melzner *et al.* [13] and 310–350 cells ml^{-1} during food-limiting experiments. This could suggest that OA alone could be impacting the aragonite microstructure [13], resulting in the observed reduced hardness and fracture toughness. Additionally, clam shells are composed solely of aragonite, and did show reduced hardness when exposed to hypercapnia at elevated temperatures [6], which is in agreement with this study when comparing the newest aragonite growth in mussel shells grown under increasing pCO_2. Seawater acidification strongly impacted the shell strength of *Mytilus californianus* veliger larvae from 5 to 8 days old [8]. Increasing pCO_2 did not, however, impact the microhardness or fracture resistance in juvenile shells of the oyster *C. virginica* [7]. Mechanical properties have been assessed through the byssal thread in *Mytilus trossulus*: with an increase in pCO_2 from 300 to 1500 µatm the individual threads broke at lower forces and extensions as a result of plaque weakening [9]. The significant impact of OA was suggested to be due to a stress on the physiology of the organism limiting the control of shell growth [7–9], which could provide the reasoning behind the impact on material properties of the *M. edulis* shell observed in this study.

The mechanical properties maps (figures 1 and 2) highlight *E*- and *H*-values of extreme significant difference at 750 µatm pCO_2. It would seem that the newest calcite in particular is significantly stiffer and harder at this level of increased pCO_2, suggesting a potential threshold for the calcitic shell at which the shell is most fragile and vulnerable to predation and changing environments. This is further supported by electron backscatter diffraction analyses of the shell of the mussel *M. edulis*, where at 750 µatm pCO_2 the shell calcite became disorientated [12]. Changes to the crystallographic control within the shell may alter the structural integrity and, in doing so, produce more fragile, brittle shells that are more vulnerable to predation. This is supported by the nanoindentaion analysis of this study and the ultrastructure analyses of Fitzer *et al.* [12], who reported diminished capacity to maintain crystallographic orientation and structural integrity under OA. It was suggested that reductions in shell integrity could result in reduced shell strength [12]; this is supported by this study with significantly reduced fracture toughness at 550 and 750 µatm.

Compensated metabolism of the proteins required for shell production was suggested to be the cause of the resultant reduced structural integrity of the mussel shells [12].

In the newest calcite growth of mussel shells, calcite is significantly stiffer and harder when grown with increasing pCO_2. However, when the same pCO_2 was combined with increasing seawater temperatures the calcite is more elastic and softer, although still significantly stiffer and harder than calcite grown in ambient conditions. Previously complex interactive effects of increasing pCO_2 and increasing temperatures have been observed to impact the physiology and biomineralization of marine bivalves [6]. Temperature was found to modulate the impact of increasing pCO_2 on the biomineralization of a clam and oyster observed in significantly increased carbonic anhydrase activity [6], which is in agreement with the findings of this study. The Earth's climate has changed over geological time with the coupling of elevated CO_2 and global increases in temperature [23]. It has been previously suggested that a return to ancestral palaeo-ocean conditions could facilitate adaptation through the return to ancestral physiologies [24] to deal with concomitant CO_2 and temperature changes. This was originally suggested for sperm swimming speeds of sea urchin larvae during palaeo-ocean conditions [24]. In this study, it could be suggested that increasing seawater temperatures predicted under global warming could buffer or reduce the impact of projected increasing pCO_2 on the material properties of the mussel shell.

5. Conclusion

OA may cause brittle shell formation with reduced fracture toughness in the mussel, *M. edulis*, which could prove problematic under environmental change and predation conditions. The highly significant increases in stiffness and hardness in the mussel shells grown under 750 µatm pCO_2 compared with ambient conditions (380 µatm) imply a potential threshold for mussel shell growth under OA. When combining the increased pCO_2 with increases in seawater temperature to ambient plus 2°C, the significance of the pCO_2 impact on the mussel shell hardness and elasticity is reduced. This might suggest that combining increased ocean pCO_2 and temperatures projected for future global ocean change may reduce the impact of increasing pCO_2 alone on the material properties of the mussel shell by returning to ancestral evolutionary mechanisms. This study highlights the need for the synergistic study of ocean global change and highlights detrimental impacts of OA on mussel shell material properties leading to increased predation and shell damage from changing environments.

Acknowledgements. Thanks to John Gilleece at the University of Glasgow for technical support.

Funding statement. This study was funded by the Leverhulme Trust project entitled 'Biomineralization: protein and mineral response to ocean acidification' awarded to M.C., N.K. and V.P.

References

1. Doney SC, Fabry VJ, Feely RA, Kleypas JA. 2009 Ocean acidification: the other CO_2 problem. *Annu. Rev. Mar. Sci.* **1**, 169–192. (doi:10.1146/annurev.marine.010908.163834)
2. Beniash E, Ivanina A, Lieb NS, Kurochkin I, Sokolova IM. 2010 Elevated level of carbon dioxide affects metabolism and shell formation in oysters *Crassostrea virginica*. *Mar. Ecol. Progr. Ser.* **419**, 95–108. (doi:10.3354/meps08841)
3. Byrne M. 2012 Global change ecotoxicology: identification of early life history bottlenecks in marine invertebrates, variable species responses and variable experimental approaches. *Mar. Environ. Res.* **76**, 3–15. (doi:10.1016/j.marenvres.2011.10.004)
4. Kamenos NA, Burdett HL, Aloisio E, Findlay HS, Martin S, Longbone C, Dunn J, Widdicombe S, Calosi P. 2013 Coralline algal structure is more sensitive to rate, rather than the magnitude, of ocean acidification. *Glob. Change Biol.* **19**, 3621–3628. (doi:10.1111/gcb.12351)
5. Thomsen J, Casties I, Pansch C, Körtzinger A, Melzner F. 2013 Food availability outweighs ocean acidification effects in juvenile *Mytilus edulis*: laboratory and field experiments. *Glob. Change Biol.* **19**, 1017–1027. (doi:10.1111/gcb.12109)
6. Ivanina AV, Dickinson GH, Matoo OB, Bagwe R, Dickinson A, Beniash E, Sokolova IM. 2013 Interactive effects of elevated temperature and CO_2 levels on energy metabolism and biomineralization of marine bivalves *Crassostrea virginica* and *Mercenaria mercenaria*. *Comp. Biochem. Physiol. A* **166**, 101–111. (doi:10.1016/j.cbpa.2013.05.016)
7. Dickinson GH, Ivanina AV, Matoo OB, Pörtner HO, Lannig G, Bocl C, Beniash E, Sokolova IM. 2012 Interactive effects of salinity and elevated CO_2 levels on juvenile eastern oysters, *Crassostrea virginica*. *J. Exp. Biol.* **215**, 29–43. (doi:10.1242/jeb.061481)
8. Gaylord B, Hill TM, Sanford E, Lenz EA, Jacobs LA, Sato KN, Russell AD, Hettinger A. 2011 Functional impacts of ocean acidification in an ecologically critical foundation species. *J. Exp. Biol.* **214**, 2586–2594. (doi:10.1242/jeb.055939)
9. O'Donnell MJ, George MN, Carrington E. 2013 Mussel byssus attachment weakened by ocean acidification. *Nat. Clim. Change* **3**, 587–590.
10. Fitzer SC, Caldwell GS, Close AJ, Clare AS, Upstill-Goddard RC, Bentley MG. 2012 Ocean acidification induces multi-generational decline in copepod naupliar production with possible conflict for reproductive resource allocation. *J. Exp. Mar. Biol. Ecol.* **418–19**, 30–36. (doi:10.1016/j.jembe.2012.03.009)
11. Kurihara H, Ishimatsu A. 2008 Effects of high CO_2 seawater on the copepod (*Acartia tsuensis*) through all life stages and subsequent generations. *Mar. Pollut. Bull.* **56**, 1086–1090. (doi:10.1016/j.marpolbul.2008.03.023)
12. Fitzer SC, Phoenix VR, Cusack M, Kamenos NA. 2014 Ocean acidification impacts mussel control on biomineralisation. *Sci. Rep.* **4**, 6218. (doi:10.1038/srep06218)
13. Melzner F, Stange P, Trübenbach K, Thomsen J, Casties I, Panknin U, Gorb SN, Gutowska MA. 2011 Food supply and seawater PCO_2 impact calcification and internal shell dissolution in the blue mussel *Mytilus edulis*. *PLoS ONE* **6**, e24223. (doi:10.1371/journal.pone.0024223)
14. Findlay HS, Kendall MA, Spicer JI, Turley C, Widdicombe S. 2008 Novel microcosm system for investigating the effects of elevated carbon dioxide and temperature on intertidal organisms. *Aquat. Biol.* **3**, 51–62. (doi:10.3354/ab00061)
15. Thomsen J, Melzner F. 2010 Moderate seawater acidification does not elicit long-term metabolic depression in the blue mussel *Mytilus edulis*. *Mar. Biol.* **157**, 2667–2676. (doi:10.1007/s00227-010-1527-0)
16. Dickson A, Sabine CL, Christian JR. 2007 *Guide to best practices for ocean CO_2 measurements*. PICES Special Publication, 3. Sidney, British Columbia: North Pacific Marine Science Organization. See http://aquaticcommons.org/1443/.
17. Yao W, Byrne RH. 1998 Simplified seawater alkalinity analysis: use of linear array spectrometers. *Deep Sea Res.* **45**, 1383–1392. (doi:10.1016/S0967-0637(98)00018-1)
18. Riebesell U, Fabry VJ, Hansson L, Gattuso J-P. 2007 *Guide to best practices for ocean acidification research and data reporting*. Luxembourg: Publications Office of European Union.
19. He L-H, Yin Z-H, van Vuuren LJ, Carter EA, Liang X-W. 2013 A natural functionally graded biocomposite

coating—human enamel. *Acta Biomater.* **9**, 6330–6337. (doi:10.1016/j.actbio.2012.12.029)
20. Lawn BR, Evans A, Marshall DB. 1980 Elastic/plastic indentation damage in ceramics: the median/radial crack system. *J. Am. Ceram. Soc.* **63**, 574–581. (doi:10.1111/j.1151-2916.1980.tb10768.x)
21. Kruzic JJ, Ritchie RO. 2003 Determining the toughness of ceramics from Vickers indentations using the crack-opening displacements: an experimental study. *J. Am. Ceram. Soc.* **86**, 1433–1436. (doi:10.1111/j.1151-2916.2003.tb03490.x)
22. Kruzic JJ, Kim DK, Koester KJ, Ritchie RO. 2009 Indentation techniques for evaluating the fracture toughness of biomaterials and hard tissues. *J. Mech. Behav. Biomed. Mater.* **2**, 384–395. (doi:10.1016/j.jmbbm.2008.10.008)
23. Royer DL. 2006 CO_2-forced climate thresholds during the Phanerozoic. *Geochim. Cosmochim. Acta* **70**, 5665–5675. (doi:10.1016/j.gca.2005.11.031)
24. Caldwell GS, Fitzer S, Gillespie CS, Pickavance G, Turnbull E, Bentley MG. 2011 Ocean acidification takes sperm back in time. *Invertebr. Reprod. Dev.* **55**, 217–221. (doi:10.1080/07924259.2011.574842)